

Development of a bunching ionizer for TOF mass spectrometers with reduced resources

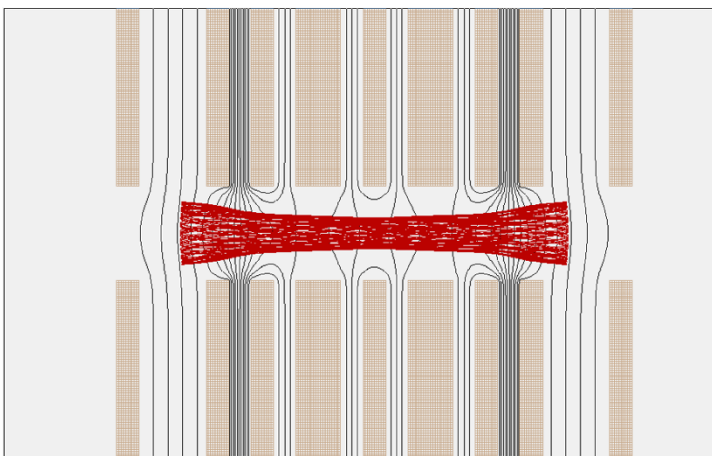
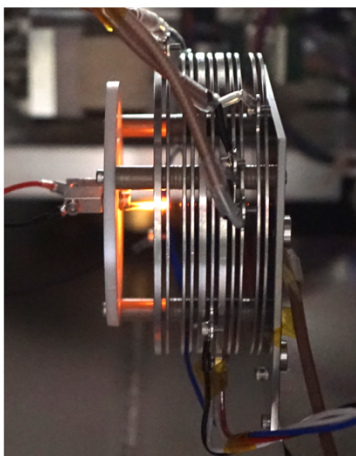
submitted to the Journal of the American Society for Mass Spectrometry (JASMS)

O. Kawashima^{*1,2}, S. Kasahara², Y. Saito^{1,2}, M. Hirahara³, K. Asamura¹, and S. Yokota⁴

¹ ISAS/JAXA, Japan ² The University of Tokyo, Japan ³ Nagoya University, Japan ⁴ Osaka University, Japan

* Corresponding author. E-mail address: kawashima.oya@jaxa.jp (Oya Kawashima)

Abstract: In some types of mass spectrometers, such as Time of Flight mass spectrometers (TOF-MSs), it is necessary to control pulsed beams of ions. This can be easily accomplished by applying a pulsed voltage to the pusher electrode while the ionizer is continuously flowing ions. This method is preferred for its simplicity, although the ion utilization efficiency is not optimized. Here we employed another pulse-control method with a higher ion utilization rate, which is to bunch ions and kick them out instead of letting them stream. The benefit of this method is that higher sensitivity can be achieved; since the start of new ions cannot be allowed during TOF separation, it is highly advantageous to bunch ions that would otherwise be unusable. In this study, we used analytical and numerical methods to design a new bunching ionizer with reduced resources, adopting the principle of electrostatic ion beam trap. The test model experimentally demonstrated the bunching performance with respect to sample gas density and ion bunching time using gas samples and electron impact ionization. We also conducted an experiment in connection with a miniature TOF-MS, and showed that the sensitivity was improved by more than one order of magnitude using the newly developed ionizer. Since the device is capable of bunching ions with lower voltage and lower power consumption (~ 100 V, ~ 0.8 W) compared with conventional RF ion trap bunchers (several kilovolts, ~ 10 W), it will be possible to find applications in portable mass spectrometer with reduced resources.



1. Introduction

A mass spectrometer (hereafter MS) can be divided into several basic parts including an ionizer, a mass analyzer, and a detector. Among them, the ionizer directly affects the performance of the MS, and thus have been well designed for laboratory and commercial use. For ionizers, as well as improving the efficiency to generate ions, efforts have been made to optimize the performance of ion optics to control the ion movement. For example, Einzel lenses, quadrupole ion lenses, and multipole-rods or stacked-rings ion guides have been adopted to maximize ion transmission efficiency to mass analyzers [1].

Types of MSs range from quadrupole, Time of Flight (hereafter TOF), magnetic, Fourier transform ion trap, RF ion trap, and other relatively minor ones. The ionizer should be optimized for each type, and the focus of this study is on TOF-MSs, which require pulsed ion current to control the timing of ion ejection (Figure 1). Basically, the timing control can be accomplished by applying pulsed voltages to a pusher electrode while an ion source is continuously streaming ions. This is essentially a loss-making operation in terms of the ion utilization. If timing information is required for mass separation, the next ejection must be stopped until the end of the analysis. Any ions that are streamed during this period are lost without being used. On the other hand, there is another popular pulse control method occasionally used in laboratory high-end equipment, where ions are bunched and kicked out instead of being streamed. The benefit of this method is that higher sensitivity can be achieved by bunching ions that would otherwise be unusable. With flexibility in controlling the amount of ions in bunching, saturation or reaching upper limit of quantitation can be avoided, making operation equivalent to that of a streaming ionizer possible.

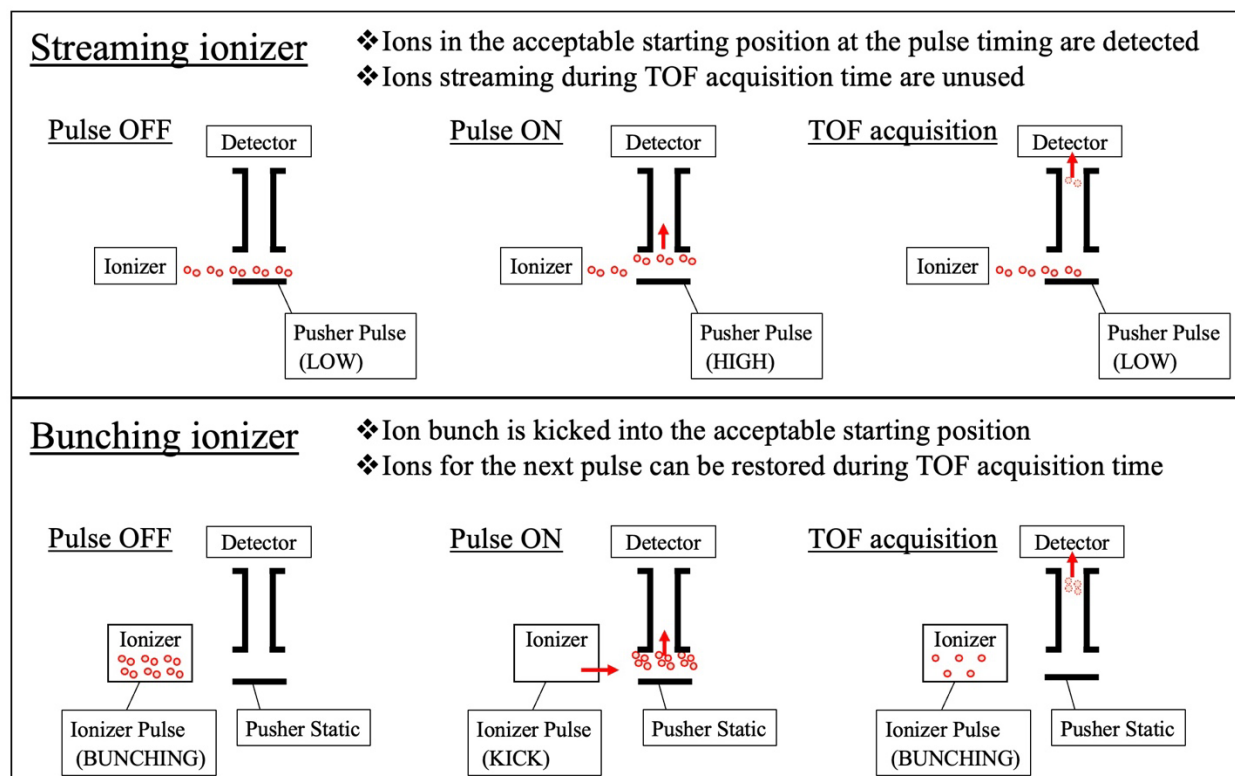


Fig. 1. Schematic diagram of TOF with static ionizers (upper) and bunching ionizers (bottom).

In general, MS performance is often a trade-off between the resources (e.g., size of the ion optics and power consumption), and therefore the sensitivity issue becomes more apparent in the development of miniaturized MSs.

There are some situations where performance should be compromised for resources. The recent increase in demand for portable MSs for environmental monitoring, for volcanic gas measurements on aircraft, and for analyses of extraterrestrial samples on spacecraft is illustrative. In such small MSs, it is better to have ionizers that compensate for the reduced sensitivity. Previous study reported that the ROSINA RTOF on board the ESA's Rosetta spacecraft employed “the electron impact storage ion source” that utilizes the slight potential drop caused by the space charge effect of the electron beam so as to retain the generated ions for a certain time [2]. When using electron impact ionization (hereafter EI), it is simplest to utilize the accompanying electron beam potential, but in order to provide a considerable potential drop such as larger than ~ 1 mV, the electron beam density must be significantly high ($> \sim 1$ A mm⁻²) [3, 4]. The electron beam density used in ordinary EI is ~ 1 mA mm⁻², which may threaten to provide insufficient potential drop compared to the stability of the power supply. Other than that, there are no reports of the use of bunching ionizers in miniature TOF-MSs despite the need for them. This is presumably because the prevailed ion bunchers are mainly designed as RF ion traps, and requires certain amount of additional resources. Examples of RF ion bunchers are found in high-end equipment such as LCMS-IT-TOFTM [5], C trap [6] and quadrupole linear ion trap [7–9]. In these instruments, by allocating additional electrical resources including a RF power supply (\sim kV amplitude and \sim MHz frequency) that generally requires 5–10 W [10], not only pulsed ion currents but also MSⁿ tandem analysis are enabled. This must be the best choice if there is room for the additional resources, but as evidenced by the lack of this option on previous small MSs, it is worthwhile to study a rather simplified buncher.

In this context, we developed a new miniature bunching ionizer which allows ionization of neutral gases and subsequent bunching at low voltage (~ 100 V) and reduced power consumption (~ 0.8 W). The ionizer can bunch ions using only DC voltages, and by applying low pulsed voltages, the bunch can be kicked out. We developed the new device based on the principle of electrostatic ion beam traps (hereafter EIBT) [11]. In section 2, we describe its design from analytical and numerical aspects. Section 3 presents the results of experimental performance tests, including bunching tests by the ionizer itself and sensitivity tests in combination with a small MS. Section 4 summarizes the results of the development and discusses the general applicability to the future instruments.

2. Design Description

2.1. Analytical expression

An EIBT is a device invented to store high-energy ion beams using DC electric field [11]. The trap can be achieved by positioning ion mirrors oppositely just as in laser cavities which keep photon beams reflecting within mirrors. The EIBT has been used in laboratory energetic charged-particle experiments, including measurements of ion lifetime and ion cooling efficiency [11, 12]. Until now, relatively large trap sizes of the EIBT design (> 230 mm) have been reported due to the intent to be suitable for such experiments.

In this study, we investigated a new set of achievable parameters of the EIBT for the purpose of resource minimization, specifically smaller size and lower voltage. The schematic image of the device is shown in Figure 2. The trap consists of two ion mirrors and two ion lenses, all of which are combinations of disk-shaped electrodes with a hole in the middle. The outermost ion mirrors are in the role of reflecting the ion beam to trap it inside, however, as shown in the upper left of Figure 2, the ion mirrors diverge the ion beam (i.e., act as convex mirrors). To cancel the beam divergence, ion lenses known as Einzel lenses are used to focus the beam on the axial direction.

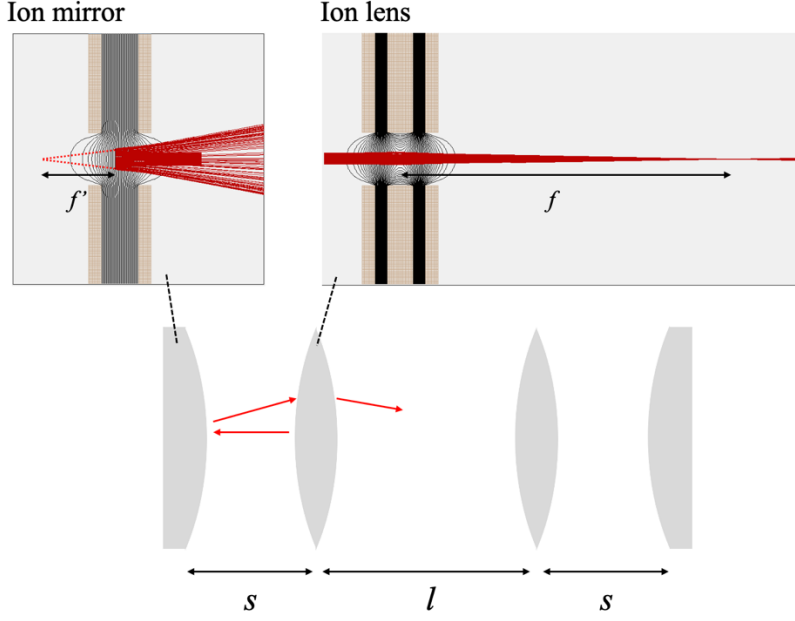


Fig. 2. Schematic of the EIBT with examples of ion beam trajectories entering ion mirrors and ion lenses. In the simulation example of the mirror and lens, ion beam trajectories are shown in red, equipotential lines are shown in black. Brown squares are cross sections of disk-shaped electrodes.

When designing a device as a combination of optical elements, ray transfer matrices are beneficial. As an analytical expression, each optical component, including free space, is described by a 2×2 ray transfer matrix that converts incoming ion-beam rays (r, θ) into outgoing rays (r', θ') . For example, an ion mirror matrix can be written as:

$$\begin{pmatrix} r' \\ \theta' \end{pmatrix} = \begin{pmatrix} 1 & 0 \\ -\frac{1}{f'} & 1 \end{pmatrix} \begin{pmatrix} r \\ \theta \end{pmatrix} \quad (1)$$

where f' is the focal length of the mirror. Similarly, an ion lens matrix can be written as:

$$\begin{pmatrix} r' \\ \theta' \end{pmatrix} = \begin{pmatrix} 1 & 0 \\ -\frac{1}{f} & 1 \end{pmatrix} \begin{pmatrix} r \\ \theta \end{pmatrix} \quad (2)$$

where f is the focal length of the lens. In addition, if we consider the field-free region of length d to be an optical element, the beam travels with an initial inclination, thus:

$$\begin{pmatrix} r' \\ \theta' \end{pmatrix} = \begin{pmatrix} 1 & d \\ 0 & 1 \end{pmatrix} \begin{pmatrix} r \\ \theta \end{pmatrix} \quad (3)$$

Considering equations (1)-(3), the transfer matrix for a half round trip in the trap, which is the minimum unit of repeated components when considering an infinite trap, is as follows:

$$\begin{aligned}
& \begin{pmatrix} 1 & 0 \\ -\frac{1}{f'} & 1 \end{pmatrix} \begin{pmatrix} 1 & s \\ 0 & 1 \end{pmatrix} \begin{pmatrix} 1 & 0 \\ -\frac{1}{f} & 1 \end{pmatrix} \begin{pmatrix} 1 & l \\ 0 & 1 \end{pmatrix} \begin{pmatrix} 1 & 0 \\ -\frac{1}{f} & 1 \end{pmatrix} \begin{pmatrix} 1 & s \\ 0 & 1 \end{pmatrix} \\
& = \begin{pmatrix} \left(1 - \frac{l}{f}\right) \left[\left(1 - \frac{s}{f'}\right) \left(1 - \frac{s}{f}\right) - \frac{s}{f} \right] - \frac{l}{f'} \left(1 - \frac{s}{f}\right) - \frac{l}{f} & \left(1 - \frac{l}{f}\right) \left(2 - \frac{s}{f'}\right) s - \frac{ls}{f'} + l \\ -\frac{1}{f} \left[\left(1 - \frac{s}{f'}\right) \left(1 - \frac{s}{f}\right) - \frac{s}{f} \right] - \frac{1}{f'} \left(1 - \frac{s}{f}\right) - \frac{1}{f} & -\frac{1}{f} \left(2 - \frac{s}{f'}\right) s - \frac{s}{f'} + 1 \end{pmatrix} \equiv K = \begin{pmatrix} A' & B' \\ C' & D' \end{pmatrix} \quad (4)
\end{aligned}$$

where the distance between the lens and the mirror is s , and the distance between two lenses is l . Here, a necessary condition for an infinite ion trap is equal to the condition that (r, θ) do not diverge after repeated manipulation of the matrix K . Translating this condition as an eigenvalue problem, we consider the following equation about eigenvalues λ of the system:

$$K \begin{pmatrix} r_0 \\ \theta_0 \end{pmatrix} = \lambda \begin{pmatrix} r_0 \\ \theta_0 \end{pmatrix} \quad (5)$$

By transforming the equation (5) using the unit matrix E , we obtain:

$$[K - \lambda E] \begin{pmatrix} r_0 \\ \theta_0 \end{pmatrix} = 0 \quad (6)$$

The determinant of each ray transfer matrix is 1, and therefore:

$$\det(K) = A'D' - B'C' = 1 \quad (7)$$

The eigenequation of the system is as follows:

$$\lambda^2 - (A' + D')\lambda + 1 = 0 \quad (8)$$

Using the expression of $\text{tr}(K) = A' + D'$, the eigenvalues are expressed as follows:

$$\lambda_{\pm} = \frac{\text{tr}(K)}{2} \pm \sqrt{\left(\frac{\text{tr}(K)}{2}\right)^2 - 1} \quad (9)$$

If $\text{tr}(K)/2$ is greater than 1, there should be an eigenvalue greater than 1. This means that vectors (r, θ) are stretched in the corresponding eigendirection by the repeated manipulation of matrix K , which causes the ions to collide with the electrodes. Therefore, the stability condition for an infinite trap is that the magnitude of both eigenvalues is less than 1, which can be expressed as:

$$\left| \frac{\text{tr}(K)}{2} \right| \leq 1 \quad (10)$$

$$\therefore 0 \leq \left(1 - \frac{s}{f}\right) \left(1 - \frac{l}{2f}\right) - \frac{1}{4f'} \left(1 - \frac{s}{f}\right) \left(2s + l - \frac{ls}{f}\right) \leq 1 \quad (11)$$

Inequality (11) shows that the ion beam trap condition can be satisfied by choosing the appropriate four parameters (s, l, f, f') . We chose $s = 10$ mm and $l = 5$ mm by setting the minimum electrode thickness at 1 mm for the manufacturing reason, and setting the minimum distance between electrodes at 1 mm for reducing discharge risks. By fixing these values, (11) is reduced to two variables, and the (f, f') region satisfying the inequality is represented by the shaded region in Figure 3. As noted above, the ion mirrors act as convex mirrors and thus the choices of parameters are limited to the red shaded regions. Of these red regions, we chose the smaller $1/f$ and $1/f'$ which can be achieved at the lower voltages. Finally, the parameters $(s, l, 1/f, 1/f') = (10, 5, 0.05, -0.2)$ or $(s, l, f, f') = (10, 5, 20, -5)$ were selected for consistency of geometrical size and focal length.

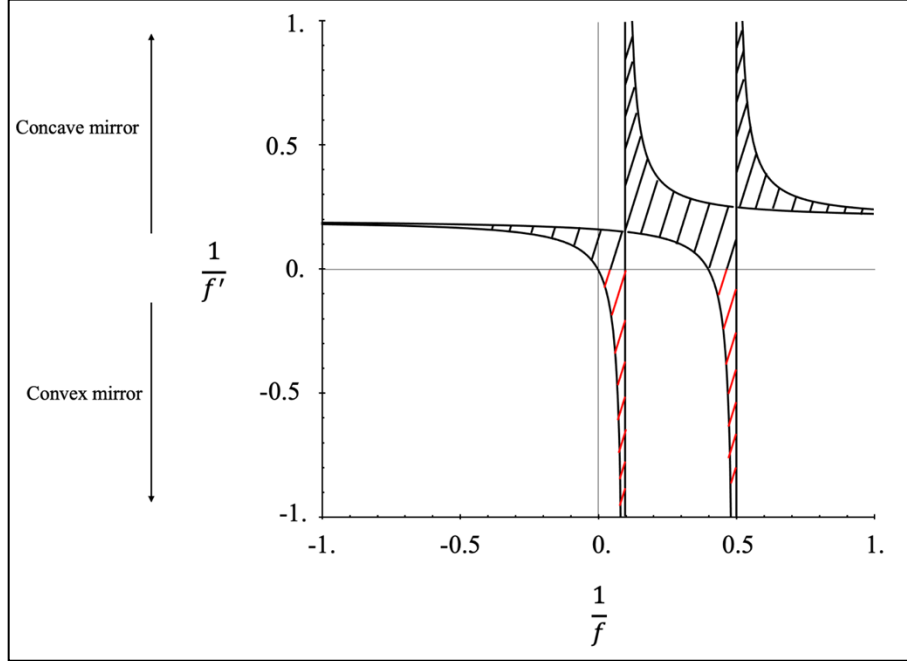


Fig. 3. Parameter region satisfying inequality (11) when $s = 10$ mm and $l = 5$ mm. The horizontal axis is the inverse of the lens focal length, and the vertical axis is the inverse of the mirror focal length.

2.2. Numerical simulation

In the following, we present the design of the EIBT optics satisfying $(s, l, f, f') = (10, 5, 20, -5)$. While s and l are parameters solely depend on geometry, f and f' depend on several variables including the geometry, the voltages of the lens and mirror, and the energy of the ion beam. To fix the geometry of the device, it is therefore necessary to determine the voltages to be used and the energy of the ion beams to be trapped.

To consider the voltages and ion beam energies, we first determined the ion trapping method. When obtaining ions inside traps, there are two choices: an external method, in which the electric potential is temporarily opened at the moment of the ion-beam entry and is immediately returned to the trapping status, or an internal method, in which ions are generated in the trappable region and are subsequently trapped. For our purposes, it is reasonable to choose the internal method to bunch ions while ionizing neutral gases. This means we needed to optimize the ionization efficiency at the trappable region. We employed EI as the ionization method, and to maximize ionization efficiency using EI, electrons with kinetic energies of 60–80 eV should be bombarded with the neutral gases [13]. Thus, we set the potential difference between the electron gun and the trappable region to 60–80 V.

Assuming a typical ion beam energy of 70 eV, numerical simulation is useful to determine the mirror and lens voltages that satisfy $(f, f') = (20, -5)$. Using SIMION® 8.0 software, we confirmed that a mirror with a combination of 80 V, 57 V, and 0 V electrodes and a lens with a combination of 0 V and 30 V electrodes satisfy these conditions. Figure 4 shows the summary of the calculations integrating these electrodes as one device. Figure 4a shows the electron beam trajectories with equipotential lines and electrodes in the new device. We employed a thermionic electron gun combined with Whenelt-type electrodes capable of ~ 10 mA mm⁻² sr⁻¹ brightness at 80 V [14]. Note that space-charge effects (i.e., contribution of point charges to electric potential) were ignored in this simulation to reduce the calculation resources. It is possible that the electron beam may become more dispersed depending on the beam density. Furthermore, we cannot rule out the possibility that the space-charge effect of the electron beam could distort the ion trapping potential and make trapping impossible; however, we report in the following section that, at

least under the experimental conditions we used, there seemed to be no such problems. Figure 4b shows the example of ion distribution during bunching. The red points show the ion positions at $10\ \mu\text{s}$ when ionizing N_2 gas of 1×10^{-4} Pa. In this calculation, the ions were assumed to be randomly produced on the electron beam trajectories in Figure 4a. The ion generation were assumed to happen during $0\text{--}10\ \mu\text{s}$ at a rate proportional to the density of the N_2 gas and the density of the electron beam. The bunched ions can be lost in collisions with the background N_2 gas, and the effects are simulated with the SIMION elastic hard sphere collision model. With this model, ions are randomly deflected at each time step with a probability depending on the neutral gas pressure. In Figure 4b, about 10% out of the generated ions were finally bunched.

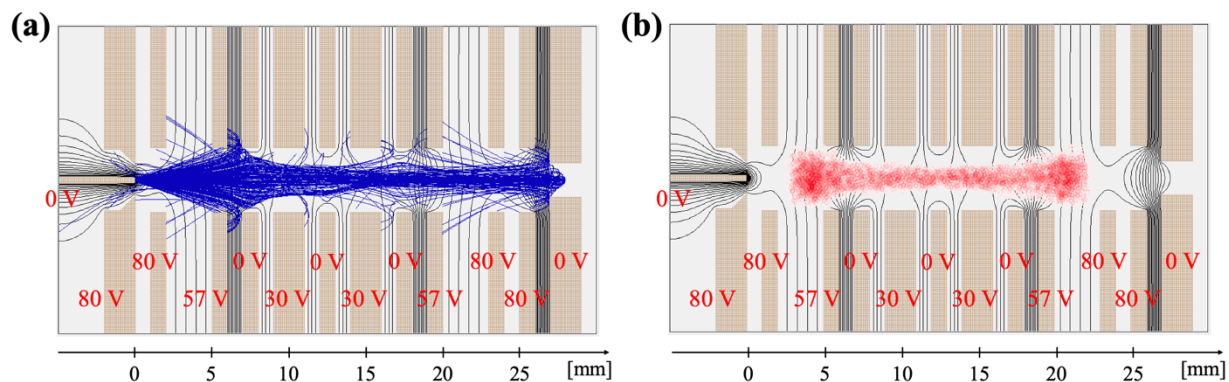


Fig. 4. (a) Electron beam trajectories (blue lines). Electrons emitted from a 0 V electron gun (left center) are accelerated and injected into the EIBT, ionizing background neutral gas. (b) Spatial distribution of ions (red points) at the moment of $10\ \mu\text{s}$ with the analyte of N_2 gas at 1×10^{-4} Pa. In both, the black lines show equipotential lines in 10 V increments, and the brown squares show cross sections of the disk-shaped electrodes. The red numbers are the voltages applied to the electrodes.

The result in Figure 4b confirm that the generated ions should accumulate successively in the EIBT. As the next step, it is equally important to verify whether the bunched ions can be kicked out toward mass analyzer. By switching the voltage from the configuration shown in Figure 4, bunched ions should be kicked out so that the timing of the TOF start can be synchronized. Figure 5 shows the calculation results simulating the kick-out, where voltage switching is triggered at $t = 10\ \mu\text{s}$. The voltage switching requires a finite time that may not be negligible; in this study, with the help of EOSTECH Ltd., Kanagawa, Japan, we used a proprietary fast switcher with a time constant of less than $\sim 10\text{ ns}$. Therefore, the calculation assumes the voltage waveform switches linearly from low to high between 10.00 to $10.01\ \mu\text{s}$. An example of ion trajectories after $10.01\ \mu\text{s}$ is shown in Figure 5a. Basically, the switched voltage is arranged such that the ions flow forward. In addition, the Wehnelt voltage is switched to -100 V to suppress the emission from electron gun, since continuous ion generation after switching is undesirable as a pulsed ion current source. Figure 5b shows a heatmap about the number of ions passing through the “Profile Plane” in Figure 5a. The distribution of ions is focused on the center owing to the lensing effect set up at the end. Figure 5c shows a kinetic energy profile of the ions at the “Profile Plane”. Basically, the ions are trapped with energies corresponding to the potential at the location where they are generated, so it is reasonable that the almost all ions are distributed within $60\text{--}80\text{ eV}$. Figure 5d shows a TOF profile of ions at the “Profile Plane”. This design facilitates the ejection of ions that were $z = 6\text{--}8\text{ mm}$ at the moment of the switch, resulting in the large peak at $10.5 \pm 0.1\ \mu\text{s}$. Note that these calculations are for N_2^+ ions ($m/z = 28$), and different mass-to-charge ratios will change the TOF and other results.

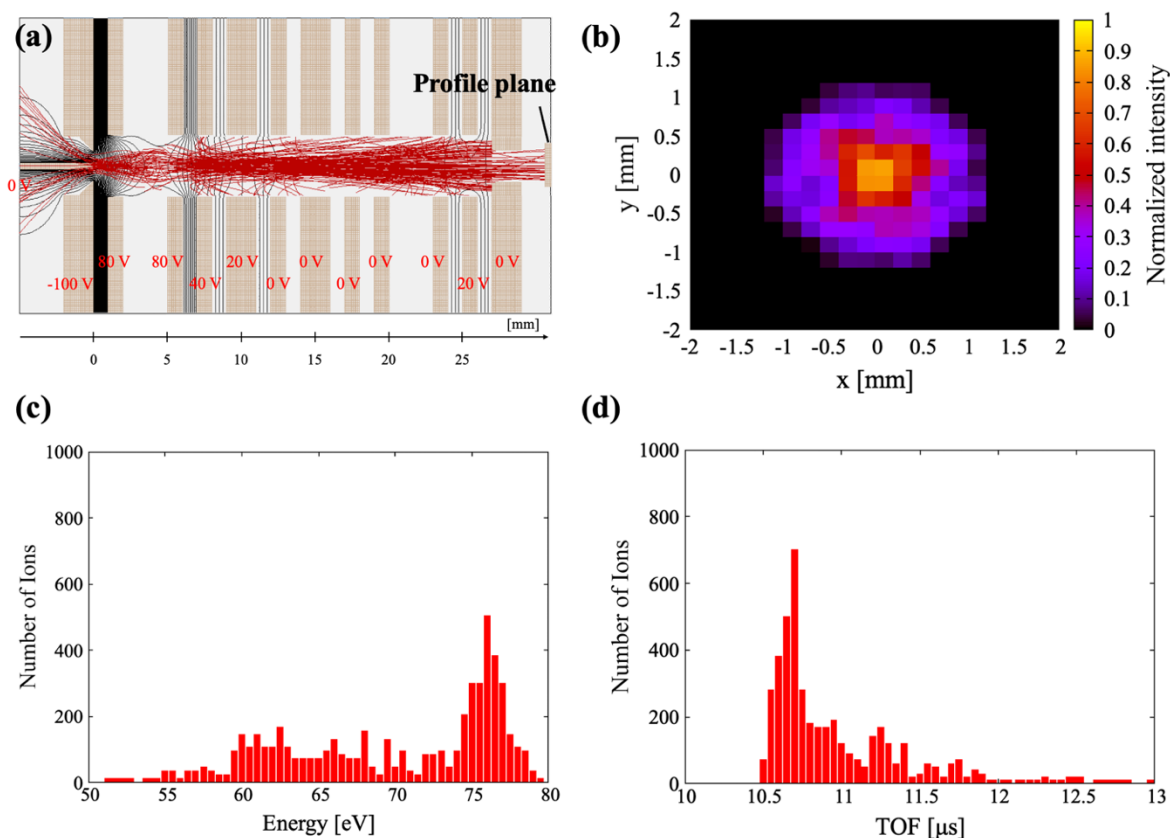


Fig. 5. Simulation to check for ion bunch kicking out. In these calculations, ions are initially distributed as shown in Fig. 4b. All results are calculated for N_2^+ ions ($m/z = 28$). (a) Ion trajectories (red lines) after voltage switching. The black lines show equipotential lines in 10 V increments, and the brown squares show cross sections of the disk-shaped electrodes. (b) A heatmap about the number of ions reaching the “Profile Plane” in Figure 5a. (c) A kinetic energy profile of the ions at the “Profile Plane”. (d) A TOF profile of ions at the “Profile Plane”.

3. Experimental results and discussion

3.1. Demonstration of ion bunching

Here we present the experimental results using a test model fabricated according to the design in Section 2. The experimental operation to demonstrate the bunching capability is shown in Figure 6. The voltage was switched between bunching mode (Mode I) and kick-out mode (Mode II). The duration of bunching mode was variable, while the duration of kick-out mode was fixed at 1 ms. In bunching mode, ions were continuously generated at the trappable region by EI, and subsequently trapped. As the analyte sample gas, pressure-regulated 99.9% dry N_2 was used. In the kick-out mode, the ion bunch was ejected, and the electron beam was suppressed by switching the Wehnelt electrode to -100 V. As noted above, voltage switching between these two modes was performed by a proprietary high-speed switcher with a time constant of less than ~ 10 ns. The switcher only required ~ 0.8 W in average during the experimental test. Considering that RF power sources for ion guides and ion traps require generally 5–10 W [10], the new bunching ionizer is consuming lower power. As a detector of the ion bunch, we used an inverting charge amplifier, which outputs a opposite polarity voltage proportional to the total amount of ions

injected. Therefore, the detector voltage at the timing of the ion bunch injection should be negative, since the EI method produce positive ions removing electrons from the neutral gases.

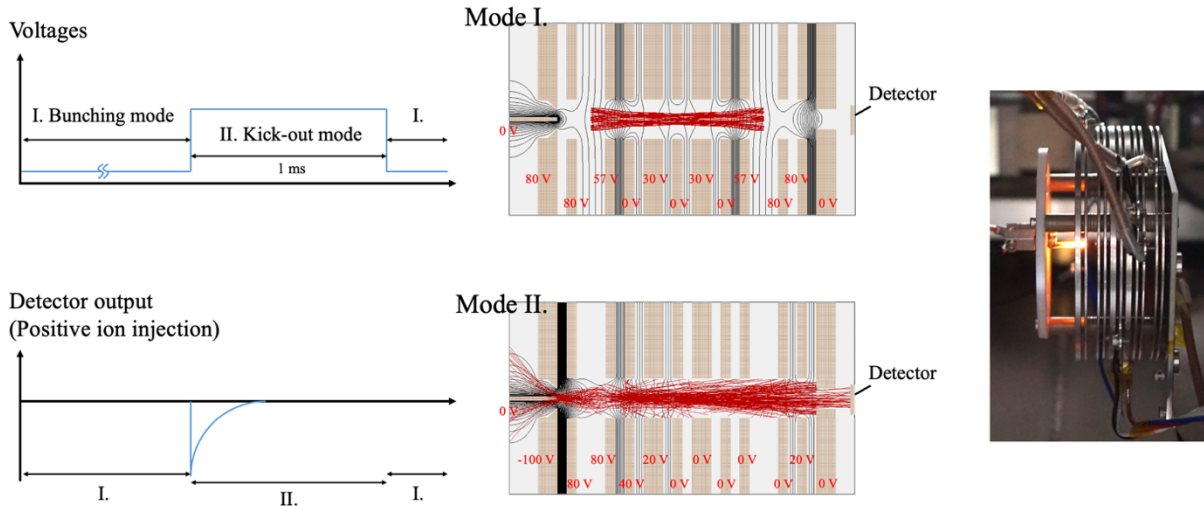


Fig. 6. The concept of experimental operation to demonstrate the bunching capability.

In Figure 7, we present an example of experimental data showing the signal of ion bunch. Figures 7a and 7b show the time series data of the detector output when Mode I is maintained for 199 ms, with a different range on the horizontal and vertical axes. On the detector output, sharp noises due to voltage switching between Mode I and Mode II appeared at the timing of 0 and 1000 μs . Other notable findings are that the pressure-dependent signal appeared from 0 μs and decayed with a time constant of $\sim 100 \mu\text{s}$, corresponding to the positive ion bunch incidence. The pressure dependency can be seen from the different amplitude of three colored lines indicating background N_2 pressure during the experiment. This result supports the basic understanding of EI, in that higher gas pressure produces more ions and therefore higher ion bunch currents.

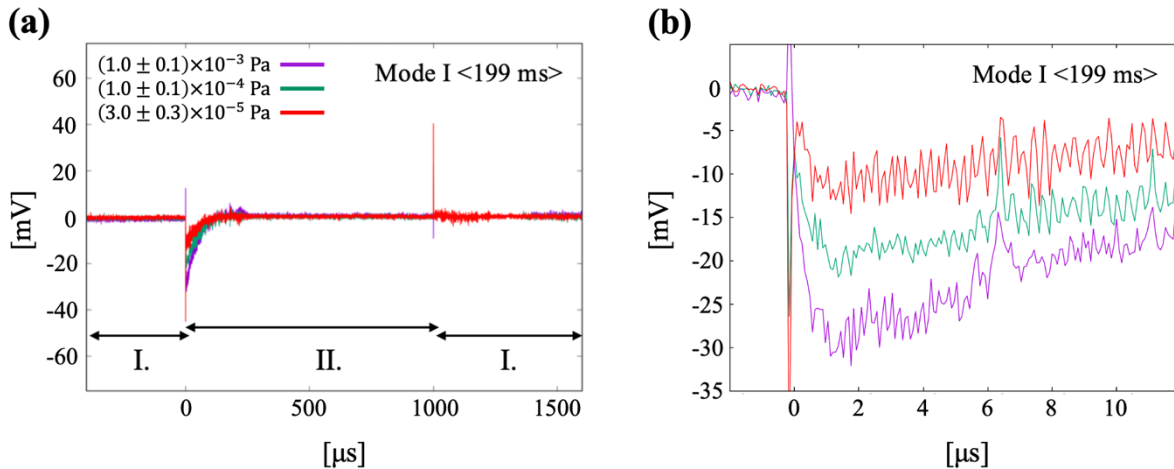


Fig. 7. An example of experimental data showing the signal of ion bunch. (a) Detector output obtained when the duration of Mode I is 199 ms. The horizontal axis shows the time, and the vertical axis shows the output voltage of the detector. Three different colored lines indicate the different pressure of N_2 gas at which the experiment was conducted, as shown in the legend. (b) Same data as in Figure 7a, but zoomed in from 0 to 10 μs on the horizontal axis and from -35 to 0 mV on the vertical axis.

Figure 8 lists the results of the data with the duration of Mode I as a variable. As a rough trend, the signal intensity increases as the Mode I time increases, which is normal given that the more ion generation time, the more ions are generated. Figure 9 summarizes these data while converting the voltages to the number of injected ions based on the calibration from oscilloscope test signals (1390 mV^{-1}). Here we can identify two phases: one in which ion abundance increases as the duration of Mode I increases ($< \sim 10^5 \mu\text{s}$), and one in which saturation occurs ($> \sim 10^5 \mu\text{s}$). The saturation can be explained by the balance between the ion production rate and the ion loss rate due to collisions with neutral particles. The ion loss rate due to neutral collisions is expressed by the following equation:

$$-dN_i = (n_g \sigma_l dz) N_i \quad (12)$$

where N_i is the number of ions considered, dz is the travel distance of ions, σ_l is the cross section for collision loss, and n_g is the number density of background neutral gases. As an order estimate, consider that the average velocity of trapped N_2^+ is of the order of 10^6 cm s^{-1} , and that n_g can be written as $n_g \sim p \times 10^{14} \text{ cm}^{-3}$ with pressure p in Pascal units. It is difficult to determine the loss cross section, but if we substitute the momentum transfer cross section between N_2^+ and N_2 ($\sigma_l \sim 10^{-16} \text{ cm}^2$) [15], the equation can be rewritten as follows:

$$-dN_i = 0.01(pt)N_i \quad (13)$$

where t is the duration of Mode I in microseconds. This means that, when t reaches $\sim 10^5 \mu\text{s}$ at the pressures of $\sim 10^{-3} \text{ Pa}$, the amount of ion loss will become comparable to total number of trapped ions. Note that the timescale estimation may change depending on the cross section, for example, that charge transfer cross section should be added, and that ions may not necessarily be lost in collisions between N_2^+ and N_2 . As more detailed estimation, the results of quantitative simulations incorporating the SIMION elastic hard sphere collision model are shown in Figure 9 by lines, which indicate the saturation timescale of 10^4 – $10^5 \mu\text{s}$ depending on the pressure. In this calculation, the collision cross section between N_2^+ and N_2 was set to $3.0 \times 10^{-16} \text{ cm}^2$ to best match the experimental results.

Another significant aspect of comparison between SIMION simulation and experimental results is that the signal was stronger than expected during the short bunching time (i.e., $< 10^3 \mu\text{s}$). These results are possibly due to an effect of electron emission overshoot. This phenomenon has been reported in various physical studies concerning the electron emissions from materials [e.g., 16]. In this case, we suspect that the sudden change in extraction voltage transferred a large number of electrons to higher energy levels in atoms, leading to a transient surge in the electron emissions from the excited materials. The simulation assumes the electron current under stable conditions; if the electron beam is temporarily larger than assumed, the ion generation rates may increase, and the ion bunch signals may become larger.

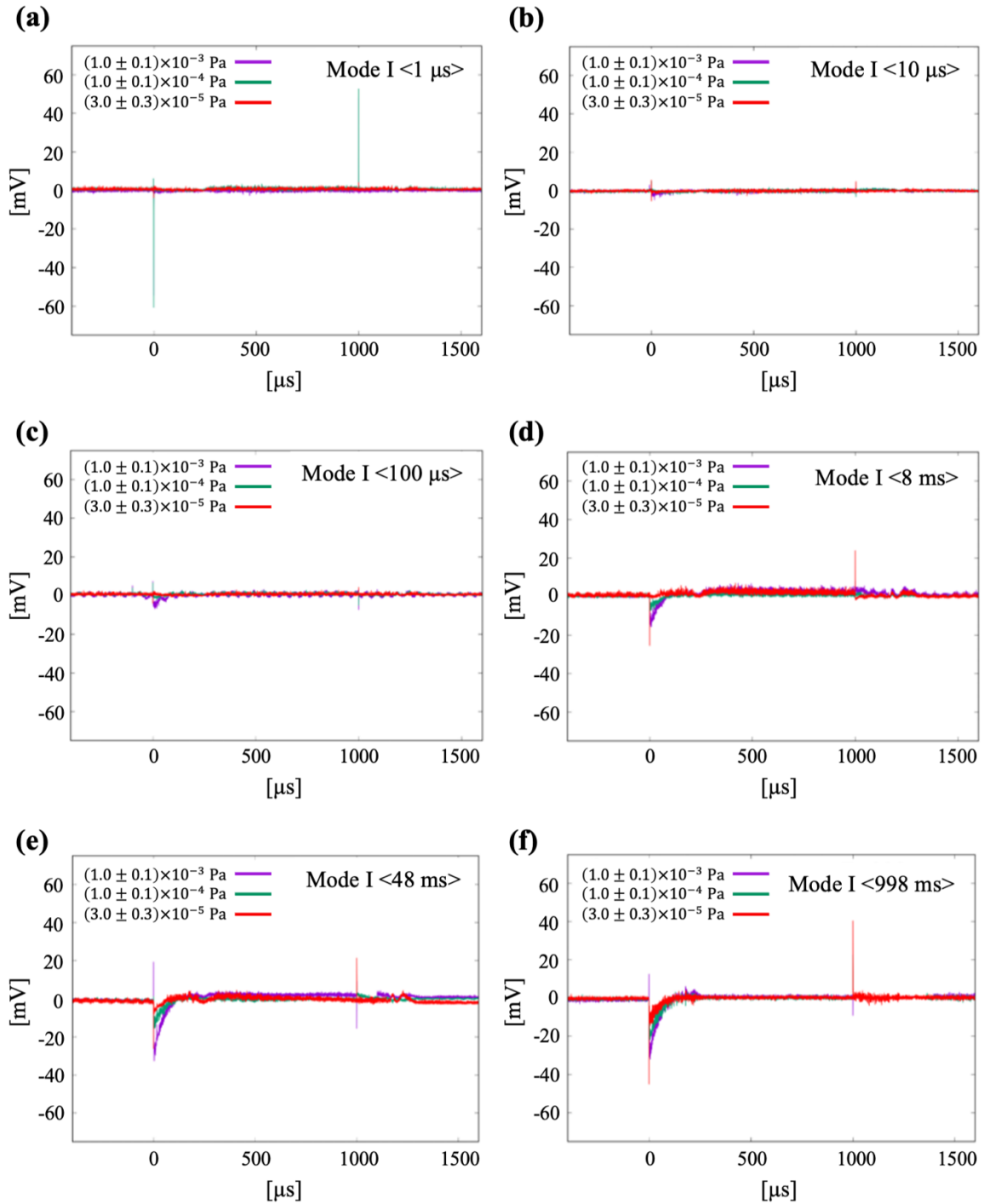


Fig. 8. Detector output obtained when the duration of Mode I is (a) 1 μ s, (b) 10 μ s, (c) 100 μ s, (d) 8 ms, (e) 48 ms, and (f) 998 ms. The horizontal axis shows the time, and the vertical axis shows the output voltage of the detector. The three different colored lines indicate the different pressures of N_2 gas at which the experiment was conducted, as shown in the legend.

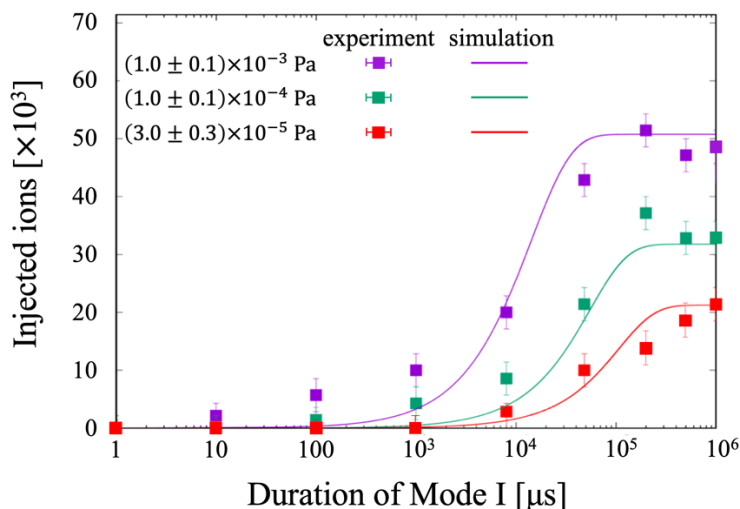


Fig. 9. Compilation of the results in Figures 7 and 8. The horizontal axis shows the duration of Mode I, and the vertical axis shows the number of injected ions. For the experimental data, points and error bars were calculated from the mean and variance of the maximum amplitude of the detector in three measurements, and the voltage output was calibrated with oscilloscope test signals. For the simulation data, pressure dependence is incorporated in the ion generation rate and in the collision frequency between N_2^+ and N_2 .

3.2. Demonstration with a miniature TOF-MS

We subsequently tested the new ion buncher in combination with a miniature TOF-MS [17] to see if this new ionizer could contribute to the sensitivity enhancement. The TOF-MS used in the experiments is a reflectron type and achieves $m/\Delta m > 50$ by sending ions back and forth within the optics. The miniature MS originally used a streaming EI ionizer to obtain the pulsed ion beam; here we conducted experimental tests by exchanging the previous ionizer to the newly developed bunching ionizer.

Figure 10 compares the experimental results with different ionizers. Both measurements were performed in a 99.9% N_2 condition at $(1 \pm 0.1) \times 10^{-4}$ Pa. The major changes in each case are the density and temporal dispersion of pulsed ion beam. For the former, increasing the density of the pulsed ion beam should contribute to an increase in sensitivity, since the expected value of the ion detection becomes higher. For the latter, temporal dispersion leads to an increase in Δm , which should result in a compromise in resolution. As expected, a remarkably positive result was achieved, where the sensitivity to N_2^+ increased by more than one order of magnitude. As a side effect, the N_2^+ peak broadened and the mass resolution decreased from $m/\Delta m \sim 50$ to 30; depending on the target gas species, we consider this compromise in resolution to be acceptable. Interestingly, there was also an increase in the intensity of the $m/z=14$ peak compared to the $m/z=28$ peak. This suggests that the ions should have encountered the electron beam several times or collided with neutral particles during the bunching time, resulting in the formation of multivalent ions N_2^{++} and fragmented ions N^+ . This demonstrates the potential for contribution to structural analysis of molecules, but also indicates that careful calibration is necessary for quantitative analysis.

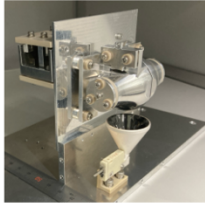
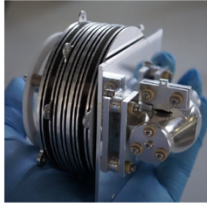
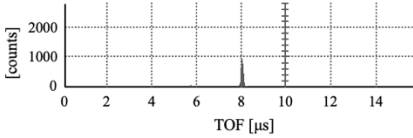
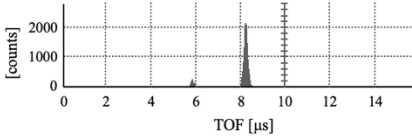
	Static Ionizer	Bunching Ionizer
		
TOF Spectrum Integration: 60 s, Analyte gas: 1×10^{-4} Pa N ₂		
Sensitivity @m/z=28 [(counts/s)/Pa]	$1.5 (\pm 0.1) \times 10^6$	$2.5 (\pm 0.1) \times 10^7$
m/Δm @m/z=28	~50	~30
[m/z=14]/[m/z=28]	0.020 ± 0.003	0.092 ± 0.010

Fig. 10. Comparison of TOF mass spectrum results obtained with different ionizers. (Left) Data obtained with a miniature TOF-MS using a streaming ionizer. (Right) Data obtained with a miniature TOF-MS using the new bunching ionizer. (First line) Examples of TOF spectrum obtained in the experiment. (Second line) Sensitivity calculated from the TOF spectrum. (Third line) Mass resolution estimated at the $m/z = 28$ peak. (Fourth line) Relative amount of ion counts for the $m/z = 14$ peak and the $m/z = 28$ peak.

4. Conclusions and outlook

In this study, we developed a new bunching ionizer based on the EIBT principle by finding new parameters suitable for miniaturization and low-voltage operation. The ionizer combines EI ionization and bunching capabilities and can store ions generated during TOF separation which are not available in streaming ionizers. The new device is small (~25 mm in length) and requires lower voltage (~100 V) and lower power (~0.8 W) than RF ion bunchers (typically several kilovolts and 5–10 W). In addition, experimental results showed that the ion bunch was obtained as expected in the simulation, and that it contributed to improved sensitivity when tested in combination with a miniature TOF-MS. Another interesting result was that the fraction of multivalent and fragment ions in the pulsed ion beam was several times higher than in the streaming ionizer.

These results indicate that the new device could be useful as an ionizer to improve the sensitivity of TOF-MSs, especially for miniature TOF-MSs with reduced resources used in harsh-environments and planetary exploration. However, when connecting this device to other TOF-MSs and using low kick-out voltages (~100 V), a time spread of ion bunch ranges of several hundred microseconds must be acceptable. Alternatively, more confined bunches could be achieved, for example, by higher kick-out voltages, post-acceleration of ion bunches, and ejecting ion bunches in a direction perpendicular to the axis. Besides sensitivity, the increase in multivalent and/or fragment ions indicates its potential use as a fragmentation/reaction cell. This can be studied as future works while considering the balance between resources and performance.

Acknowledgements

The authors gratefully acknowledge the support for text readability provided by University of Maryland. This work was supported by Kakenhi 23KJ2212, 22K2134.

Declarations

Conflict of interest: The authors declare no competing interests.

References

- [1] Li, C., Chu, S., Tan, S., Yin, X., Jiang, Y., Dai, X., ... & Tian, D. (2021). Towards higher sensitivity of mass spectrometry: a perspective from the mass analyzers. *Frontiers in chemistry*, 9, 813359.
- [2] Balsiger, H. et al. Rosina – Rosetta Orbiter Spectrometer for Ion and Neutral Analysis. *Space Science Reviews* 128, 745–801 (2007) doi: 10.1007/s11214-006-8335-3
- [3] Currell, Fred, and Gerd Fussmann. "Physics of electron beam ion traps and sources." *IEEE Transactions on Plasma Science* 33.6 (2005): 1763-1777.
- [4] Lu, Xiaojun, and F. J. Currell. "Numerical simulation of the charge balance and temperature evolution in an electron beam ion trap." *Physical Review Special Topics—Accelerators and Beams* 12.1 (2009): 014401.
- [5] Shimadzu Scientific Instruments (2009) "Advantages of LCMS-IT-TOF Mass Spectrometry in Identifying Polymer Additives" [White Paper]
- [6] Zubarev, Roman A., and Alexander Makarov. "Orbitrap mass spectrometry." (2013): 5288-5296
- [7] Brickerhoff, William B., et al. "A Dual Source Ion Trap Mass Spectrometer for the Mars Organic Molecule Analyzer of ExoMars 2018." 43rd Annual Meeting of the Division of Planetary Sciences. No. GSFC. CP. 5097.2011. 2011.
- [8] R Arevalo Jr. et al., Advanced Resolution Organic Molecule Analyzer (AROMA): Simulations, Development and Initial Testing of a Linear Ion Trap-Orbitrap Instrument for Space. 3rd International Workshop on Instrumentation for Planetary Missions (2016) 4072.pdf
- [9] Goesmann, Fred, et al. "The Mars Organic Molecule Analyzer (MOMA) instrument: characterization of organic material in martian sediments." *Astrobiology* 17.6-7 (2017): 655-685.
- [10] Jones, Ronald M., Dieter Gerlich, and Scott L. Anderson. "Simple radio-frequency power source for ion guides and ion traps." *Review of scientific instruments* 68.9 (1997): 3357-3362.
- [11] Zajfman, D., Heber, O., Vejby-Christensen, L., Ben-Itzhak, I., Rappaport, M., Fishman, R. and Dahan M. (1997) Electrostatic bottle for long-time storage of fast ion beams. *Phys. Rev. A*, 55, pp. R1577-R1580.
- [12] Dahan, M., Fishman, R., Heber, O., Rappaport, M., Altstein, N., Zajfman, D., & Van Der Zande, W. J. (1998). A new type of electrostatic ion trap for storage of fast ion beams. *Review of Scientific instruments*, 69(1), 76-83.
- [13] Engel, A.V. (1965) *Ionized gases: second edition*, Clarendon press.
- [14] Kawashima, O. et al., Development of an electron impact ion source with high ionization efficiency for future planetary missions. *Planet. and Space Sci.*, 220, 105547 (2022) doi: 10.1016/j.pss.2022.105547
- [15] Phelps, Av V. "Cross sections and swarm coefficients for nitrogen ions and neutrals in N₂ and argon ions and neutrals in Ar for energies from 0.1 eV to 10 keV." *Journal of Physical and Chemical Reference Data* 20.3 (1991): 557-573.
- [16] Chandra, V. K., et al. "Modeling of transient electroluminescence overshoot in bilayer organic light-emitting diodes using rate equations." *Journal of luminescence* 132.6 (2012): 1532-1539.

[17] Kawashima et al. "Development of an Ultra-small Mass Spectrometer for Future Lunar and Planetary Exploration." *2024 IEEE Aerospace Conference*. IEEE, 2024.